

Rho Signaling Pathway and Apical Constriction in the Early Lens Placode

Ricardo Moraes Borges,¹ Marcelo Lazzaron Lamers,² Fabio Luis Forti,³ Marinilce Fagundes dos Santos,¹ and Chao Yun Irene Yan^{1*}

¹Department of Cell and Developmental Biology, Institute of Biomedical Sciences, University of São Paulo, São Paulo, SP, Brazil

²Departamento de Ciências Morfológicas do Instituto de Ciências Básicas da Saúde, Universidade Federal do Rio Grande do Sul, Brazil

³Departamento de Bioquímica, Instituto de Química, Universidade de São Paulo, São Paulo, Brazil

Received 18 October 2010; Revised 5 January 2011; Accepted 16 January 2011

Summary: Epithelial invagination in many model systems is driven by apical cell constriction, mediated by actin and myosin II contraction regulated by GTPase activity. Here we investigate apical constriction during chick lens placode invagination. Inhibition of actin polymerization and myosin II activity by cytochalasin D or blebbistatin prevents lens invagination. To further verify if lens placode invaginate through apical constriction, we analyzed the role of Rho-ROCK pathway. Rho GTPases expression at the apical portion of the lens placode occurs with the same dynamics as that of the cytoskeleton. Overexpression of the pan-Rho inhibitor C3 exotoxin abolished invagination and had a strong effect on apical myosin II enrichment and a mild effect on apical actin localization. In contrast, pharmacological inhibition of ROCK activity interfered significantly with apical enrichment of both actin and myosin. These results suggest that apical constriction in lens invagination involves ROCK but apical concentration of actin and myosin are regulated through different pathways upstream of ROCK. *genesis* 00:1–12, 2011. © 2011 Wiley-Liss, Inc.

Key words: lens placode; epithelial Invagination; apical cell constriction; Rho GTPase; morphogenesis

INTRODUCTION

The developing eye is privileged amongst all the other embryonic tissues with an anatomical localization that facilitates its experimental manipulation and imaging, properties that have contributed to its establishment as

a classical experimental paradigm in developmental biology. The study of its development has contributed to our understanding of various issues pertinent to the field. In particular, the various morphological changes that the lens placode undergoes at different stages of development illustrate its usefulness as a model system for embryonic morphogenesis.

In brief, prior to the appearance of the placodes, the cells of the head ectoderm are cuboidal. After the molecular events that lead to the induction of the lens placode (reviewed in Donner *et al.*, 2006), the cells elongate and the placode can be identified as a flat thickened pseudo-stratified columnar structure in the head ectoderm overlying the optic vesicle. Thereafter, the cell apical/basal surface ratio decreases and the cells assume a conical shape. This results in the inward bending of placode, forming an initial shallow concavity which deepens into the lens pit as invagination progresses (Schook, 1980b). The pit expands dorsal-ventrally so as to involve the whole placode in an

Additional Supporting Information may be found in the online version of this article.

*Correspondence to: Chao Yun Irene Yan, Departamento de Biologia Celular e do Desenvolvimento, Instituto de Ciências Biomédicas, Universidade de São Paulo, São Paulo, SP 05508-000, Brazil.

E-mail: ireneyan@usp.br

Contract grant sponsor: FAPESP; Contract grant number: 2007/57450-7; Contract grant sponsor: CNPq; Contract grant number: 47.5752/06-6; Contract grant sponsor: FAPESP

Published online in Wiley Online Library (wileyonlinelibrary.com).

DOI: 10.1002/dvg.20723

invaginating event. After the ingression of the whole placode toward the underlying optic cup, the edges fuse and detach from the surface ectoderm, forming the lens vesicle (Schook, 1980b).

A variety of mechanisms have been suggested to contribute to the initial inward buckling of the placode, such as differential cell proliferation or death, tissue interaction, planar pressure derived from lateral growth and apical constriction (Hendrix *et al.*, 1993; Plageman *et al.*, 2010; Schook, 1980a; Wrenn and Wessels, 1969). Apical constriction (AC) is an evolutionary conserved phenomena that has been extensively characterized in a variety of epithelial bending events in metazoan embryogenesis, such as in cell shape changes during sea-urchin, *Drosophila* and *Xenopus* gastrulation, vertebrate neural plate and placodal bending (Barrett *et al.*, 1997; Beane *et al.*, 2006; Dawes-Hoang *et al.*, 2005; Fox and Peifer, 2007; Kinoshita *et al.*, 2008; Lee and Harland, 2007; Nikolaidou and Barrett, 2004; Plageman *et al.*, 2010; Sai and Ladher, 2008). The main driving force of AC is the contraction of apically localized acto-myosin cytoskeleton. The mechanical force generated drives reduction of the apical surface area and converts cuboidal/columnar cells into wedge-shaped cells. The coordinated occurrence of this single cell-shape change across the planar epithelium cell layer, together with the increased intercellular adhesion conferred by the enrichment of adhesive junctions, results in the bending of the flat epithelium.

The molecular mechanisms that regulate apical constriction have been extensively studied in *Drosophila* mesodermal invagination (Lecuit and Lenne, 2007) and in vertebrate neural tube closure (Haigo *et al.*, 2003; Nishimura and Takeishi, 2008; Hildebrand and Soriano, 1999). In the former, the future mesoderm invaginates and detaches from the ventral blastoderm epithelia. This process is initiated with the binding of the secreted ligand Fog to its receptor Concertina, which in turn activates Rho1/RhoA through RhoGEF2 (Barrett *et al.*, 1997; Costa *et al.*, 1994). Rho1/RhoA then activates the Rho-dependent kinase Drok/ROCK, which phosphorylates and initiates myosin II contractile activity. Inhibition of Drok/ROCK activity interferes with myosin II recruitment to the apical region, and consequently abolishes mesodermal invagination (Dawes-Hoang *et al.*, 2005; Nikolaidou and Barrett, 2004; Pilot and Lecuit, 2005).

Apical constriction in vertebrates also depends on ROCK (Haigo *et al.*, 2003; Kinoshita *et al.*, 2008). Inhibition of ROCK activity reduces the apical levels of phosphorylated myosin II and impairs AC in avian neural tube and MDCK kidney epithelial cell line (Hildebrand, 2005; Kinoshita *et al.*, 2008; Nishimura and Takeichi, 2008). Here, we confirm that apical constriction contributes toward the initial bending of the chick lens placode. Moreover, we show that GTPases play an important role in the proper placement of apical actin and myosin prior to AC in this experimental paradigm. Simi-

lar to previously-identified AC-driven epithelial morphogenesis, the distribution of both apical actin and myosin in lens placode also require ROCK activity. However, further investigation of the signaling involved in the regulation of AC indicates that actin and myosin II are differentially regulated by components upstream to ROCK. Accumulation of apical myosin II is abnormal with C3-exotoxin-mediated inactivation of RhoGTPases, whereas actin is unaffected by the same treatment.

RESULTS

Actin Filaments Colocalize With Myosin II at Apical Portion Prior to and During Lens Placode Invagination

Reduction of apical surface through myosin II-mediated contraction of apical actin network is associated with specific changes in cytoskeletal architecture (Baumann, 2004; Dawes-Hoang *et al.*, 2005; Hildebrand 2005): First, actin and myosin accumulate in the apical region where reduction of cell surface area will occur. Specifically in AC-driven events, this accumulation precedes onset of invagination. Finally, inhibition of actin-myosin function interferes with epithelial invagination by preventing apical constriction.

To address whether chick lens placode goes through the same process during its invagination, we first investigated the dynamics of actomyosin cytoskeleton localization prior to and during lens placode invagination. In particular, we analyzed three different stages of lens placode morphogenesis: pre-placodal ectoderm, early lens placode prior to invagination and invaginating placode. Pre-placodal cells are cuboidal, morphologically indistinguishable from the surrounding ectoderm and do not present a clear elongated apico-basal polarity (Byers and Porter, 1964; Fig. 1). In contrast, the early placode is a prominently thickened region composed of a single layer of pseudostratified columnar cells. Thereafter, the placode initiates the process of invagination. Morphologically this can be identified by an initial inward bending step which forms a central dimple.

Pre-placode ectoderm cells present both F-actin and myosin II homogeneously distributed at the baso-lateral and apical domains (Fig. 1a-c). In the early placode, labeling for actin at the apical side is significantly increased relative to the basal signal. This increase was detectable prior to invagination (Fig. 1d-f), persisted at the initial bending step (Fig. 1g-i) and also throughout its invagination (data not shown). In contrast, in the ectoderm that surrounds the placode, which does not invaginate, the pattern of F-actin and myosin II staining remained similar to that of pre-placode ectoderm and did not present apical accumulation of contractile elements in any of the stages analyzed (Fig. 1j-l). Quantification of the fluorescence intensity at each stage

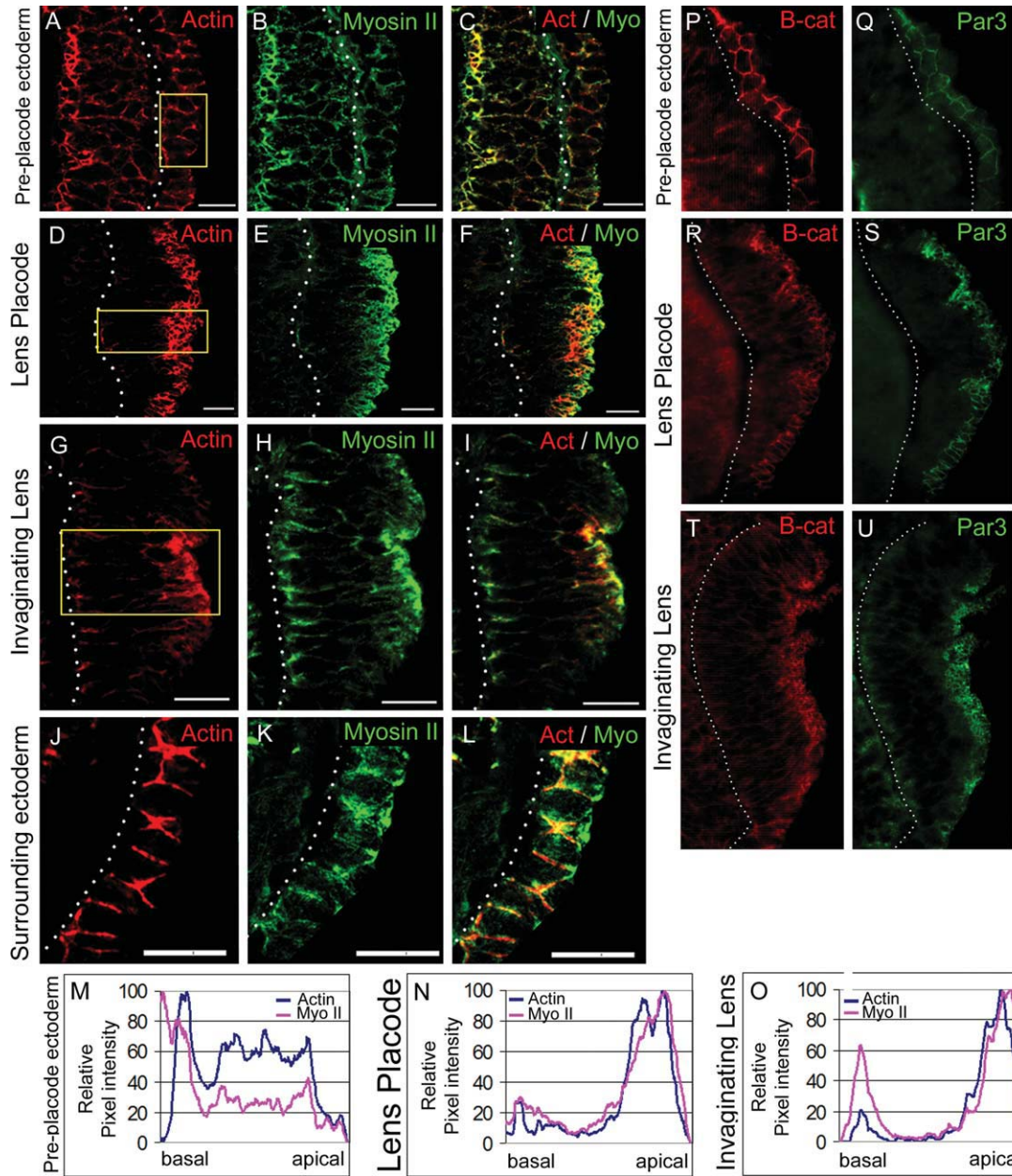


FIG. 1. Accumulation of filamentous actin and myosin II at the apical portion precedes lens placode invagination. Phalloidin-stained f-actin (a,d,g,j) and immunohistochemistry to myosin II (b,e,h,k) in dorso-ventral sections of different stages of lens development: pre-placode ectoderm (a–c); early lens placode (d–f); early steps in lens placode invagination (g–i); ectoderm surrounding invaginating lens (j–l). In all pictures, apical side of the lens is to the right, basal is to the left and dorsal is up. Dotted lines delineate lens basal portion. F-actin and myosin II are homogeneously distributed at basal, lateral and apical cell sides in the pre-placodal ectoderm (a–c). At the elongated early placode stage, actomyosin filaments become enriched at the apical side (d–f). Actomyosin filaments remain apically enriched after invagination onset (g–i). In contrast to invaginating lens, actomyosin filaments never accumulate apically in the surrounding epithelium (j–l). The dynamics of the actomyosin distribution are confirmed with the quantification of the pixel values in the boxes at each stage (m–o). The concentration of adhesive junctions (as seen by beta-catenin staining) and the polarity marker PAR-3 in the apical domain occurs with the same dynamics as actin (p–u). Bar = 20 μ m.

confirms these results (Fig. 1m–o) and reveals that myosin II also accumulates at the basal region of the invaginating lens, albeit at a lower intensity than in the apical side (Fig. 1m–o). These data suggest that apical concentration of actomyosin filaments is part of a polarization

process restricted to the placode that precedes its bending. In confirmation of this, establishment of apical adhesive junctions and distribution of the apical polarity marker PAR-3 (Afonso and Henrique, 2006) occur with a dynamics similar to actin (Fig. 1p–u).

F-actin and Myosin II are Both Necessary for Lens Placode Invagination

To confirm that the apical actin network in early placodes participates actively in the early events of its invagination, we analyzed the distribution dynamics of Phosphorylated Myosin Light Chain (p-MLC) in the same developmental stages. Phosphorylation of MLC at serine 19 increases myosin II filament formation, ATPase activity, actomyosin filaments contraction and is indicative of its activation (Kamisoyama *et al.*, 1994). In the pre-placodal ectoderm, p-MLC staining pattern is congruent with that of total myosin II. At this stage, p-MLC is homogeneously distributed in basolateral and apical submembrane regions (Fig. 2a-c). However, in the placode, apical enrichment of p-MLC is delayed in relation to total myosin II (compare Fig. 1e with Fig. 2b). We could only detect apical enrichment of p-MLC after the initial bending step has occurred, but not in the columnar lens placodal cells (Fig. 2b,c). This delay could indicate that myosin II activation occurs after bending, in which case it is not necessary for this step. Alternatively, phosphorylation of myosin could be required for bending, but occur immediately prior to its onset and thus temporarily indistinguishable from it. To distinguish between these two scenarios, we cultured head explants obtained at early placode stage in the presence of the myosin II inhibitor blebbistatin. Blebbistatin is a non-competitive inhibitor that interferes with actomyosin crosslinking by blocking myosin II in its actin-detached state (Kovács *et al.*, 2003; Straight *et al.*, 2003). After 24 h in culture, normal lens invagination occurred in 82% ($n = 28$) of control explants, while only 3% ($n = 31$) of lens placodes cultured with blebbistatin invaginated (Fig. 2). The remainder was arrested in the early placode stage, without any signs of bending or invagination. The data indicate that activity of apical myosin is essential for lens placode morphogenesis.

Likewise, local inhibition of F-actin polymerization also interfered with the invagination process. *In ovo* treatment of 18-somite stage embryos with Cytochalasin D (CD), a chemical that blocks polymerization and elongation of actin, arrested lens morphogenesis at the early placode stage in 35% ($n = 20$, at $1.5 \mu\text{g ml}^{-1}$ CD dose) of the embryos, whereas 100% of control embryos (Saline $n = 8$ or DMSO-treated $n = 20$) had normal invaginated lenses. This effect was dose dependent. The proportion of embryos with arrested placodes increased to 56% ($n = 14$) with $2.5 \mu\text{g ml}^{-1}$ CD and 69% ($n = 16$) with $5 \mu\text{g ml}^{-1}$ CD (Fig. 3b-d,h and data not shown).

The above mentioned pharmacological agents could also decrease cell proliferation or increase cell death, both of which would adversely affect lens invagination. We did not observe a significant decrease in total cell or phospho-histone H3-positive cell numbers in CD-treated placodes (Supporting Information Fig. 1). To exclude

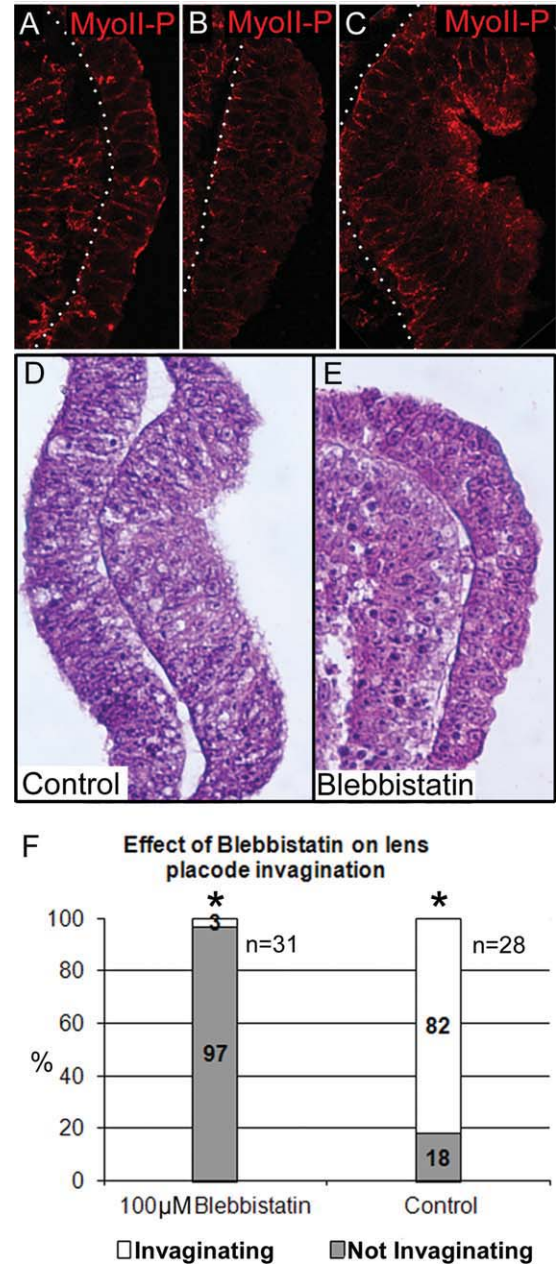


FIG. 2. Phospho-myosin II is present in lens placode and its activity is necessary for invagination. Phosphorylated myosin II is present at cell basal, lateral, and apical sides in pre-placode ectoderm and early lens placode cells (a,b). Phosphorylated myosin II was detected apically only after invagination onset (c). Hematoxylin-Eosin stained paraffin sections of placodes cultured with 100 μM blebbistatin (e) and with DMSO as control (d). Apical side of the lens is to the right, basal is to the left and dorsal is up. Lens invagination was inhibited in 97% ($n = 31$) of embryos treated with blebbistatin, while only 18% ($n = 28$) of control embryos had lenses arrested at lens placode stage (f). The difference between control and blebbistatin-treated embryos was statistically significant (*) $P < 0.001$.

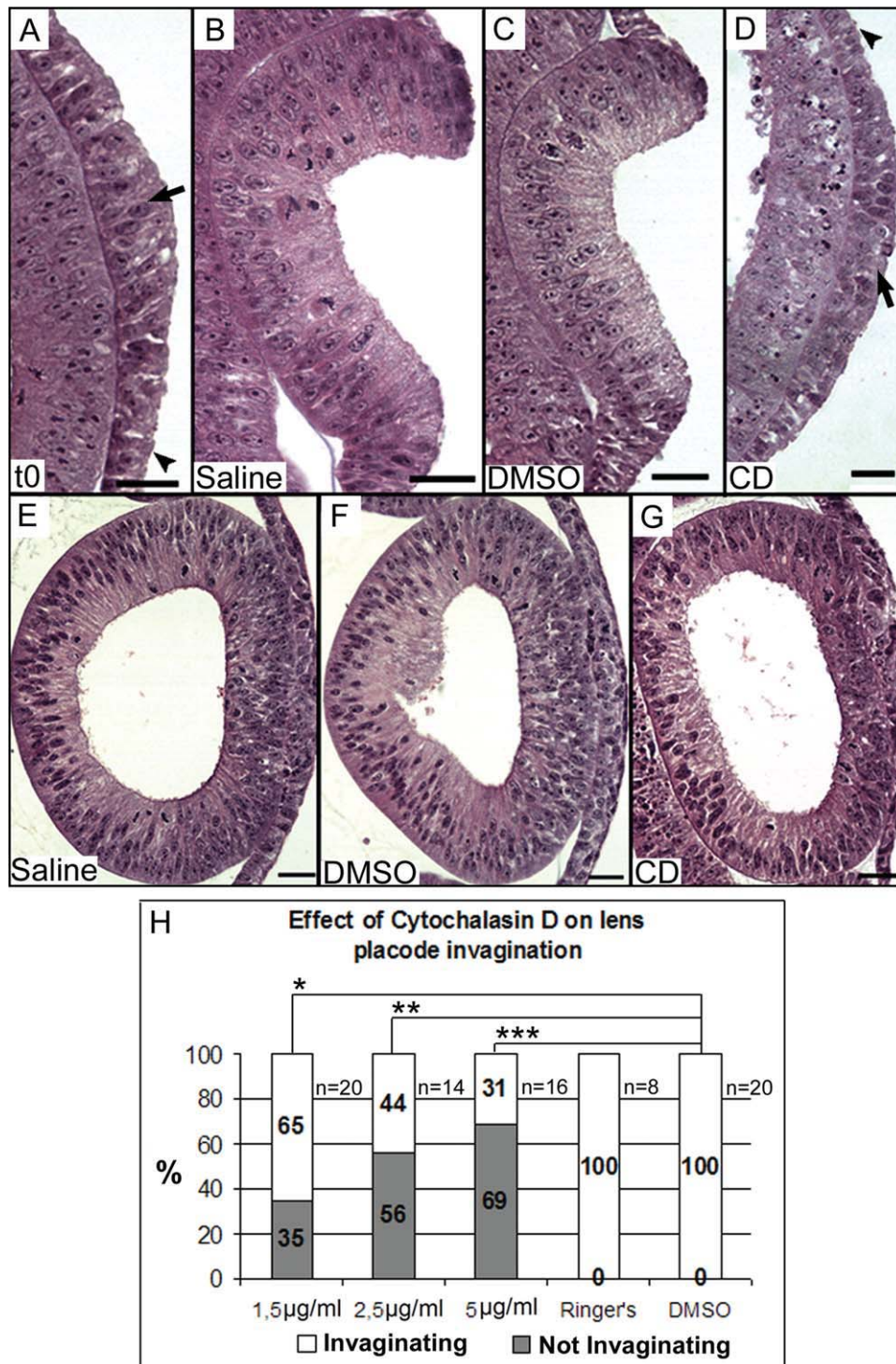


FIG. 3. Filamentous actin is necessary for lens placode invagination. (a) Hematoxylin-Eosin stained paraffin section of a typical 18 somite embryo, showing that at this stage the thickened early lens placode is already formed. Embryos at this stage were treated *in ovo* with CD (d), control Ringer's solution (b) or DMSO (c) and incubated for 6 h. When embryos were treated with $2.5 \mu\text{g ml}^{-1}$ CD, 56% of the placodes did not invaginate (d,h) ($n = 14$), while 100% of Ringer's ($n = 4$) and 100% of DMSO ($n = 20$) control embryos had the normal invaginating placodes (b,c,h). Arrow in a and d indicate the thickened placode in comparison to the surrounding ectoderm (arrowhead). The effect of CD was reversible. Embryos pre-treated with $2.5 \mu\text{g ml}^{-1}$ CD that had the lens arrested at placode stage were rinsed with saline and reincubated for 12 h to test for toxicity effects (g; $n = 7$). These embryos recovered and resumed invagination to a degree comparable to that of controls (e,f). (h) Histogram of the dose-dependent effect of CD on invagination. In all pictures, apical side of the lens is to the right, basal is to the left and dorsal is up. Bar = $20 \mu\text{m}$. *, **, *** denote a statistically significant difference relative to control of $P < 0.05$.

the possibility that the effect of CD treatment was through an increase in placodal cell death, we performed drug washout experiments. Embryos treated for 6 h with $2.5 \mu\text{g ml}^{-1}$ CD that presented placodes arrested in the pre-invagination stage were rinsed with saline solution to remove CD and reincubated for further 12 h. After reincubation, 100% ($n = 7$) of the lens placode invaginated and formed lens vesicles that detached from the overlying ectoderm at the appropriate stage (Fig. 3e–g). In addition, after CD treatment, although we did observe a slight increase in the number of picnotic nuclei in the optic vesicle, these were not detected in the lens placode. Thus, we exclude the possibility that our phenotype is generated by a toxic effect of the drugs and conclude that these data indicate that both actin filament polymerization and myosin II activity are necessary for lens placode invagination process and further supports the hypothesis that apical cell constriction drives lens placode bending.

ROCK Activity is Required for Apical Placement of Actin and Myosin II

Serine 19 in myosin II is directly phosphorylated by the Rho-dependent kinase (ROCK) (Amano *et al.*, 1996). Furthermore, both apical localization and contraction of the actomyosin cytoskeleton have been previously attributed to ROCK in a variety of morphogenetic events (BurrIDGE and Wennerberg, 2004; Dawes-Hoang *et al.*, 2005; Kinoshita *et al.*, 2008; Simoes *et al.*, 2006). When we cultured chicken embryo cephalic explants with Y27632, a pharmacological inhibitor of ROCK, lens invagination occurred in only 28% ($n = 43$) of the explants (Fig. 4e–i). In contrast, 86% ($n = 22$) of lens cultured under control conditions invaginated (Fig. 4a–d,i). When we analyzed the ratio between apical and basal fluorescence intensity in control and Y27632-treated placodes, we observed that Y27632 reduced the difference between the highest fluorescent signal at the apical domain and at the basal compartment for both actin and myosin. In control situations, the ratio between apical and basal peak signals was 100/53 for myosin and 100/7 for actin (Fig. 4j,k). Conversely, in Y27632-treated placodes the ratios decreased to 40/100 in the case of myosin and 100/99 for actin. The inhibitory effect of Y27632 on invagination was reversed after washout in 68% ($n = 19$) of the embryo explants. Likewise, the apical and basal distribution of actin filaments and myosin II were also restored to the normal pattern (Fig. 4l).

Rho GTPase is Apically Located and its Activity is Required for Accumulation of Apical Myosin

Since the chick embryo expresses three subtypes of RhoGTPases with high degree of similarity, we used a pan-Rho antibody to examine the distribution of RhoGT-

Pases during lens development (Liu and Jessell, 1998). Similarly to what we observed with the actomyosin cytoskeleton, Rho is homogeneously distributed in the pre-placode ectoderm and becomes apically concentrated in early placode prior to bending (Fig. 5a,b). Confirming a previous report, this pattern is maintained during lens pit formation (Fig. 5c; Kinoshita *et al.*, 2008). To verify if Rho GTPase activity is required for invagination, we tested the effect of *Clostridium botulinum* toxin C3 transferase overexpression in chick embryo pre-placode ectoderm by electroporation of C3 construct into one side of chick head ectoderm, leaving the contralateral side as the control. C3 directly inactivates all isoforms of Rho GTPases through ADP ribosylation (reviewed at Wilde and Aktories, 2001). Overexpression of C3 inhibited lens invagination in 77.7% ($n = 9$) of embryos (Fig. 5h), while 100% of the contralateral lens invaginated normally (Fig. 5d). Consistent with the role of Rho in establishment of adhesive junctions (Popoff and Geny, 2009) in some cases overexpression of C3 caused lens cells dissociation and detachment (data not shown). These embryos were not included in our final analysis.

In light of the multiple regulatory roles associated with Rho GTPases, C3-mediated reduction of invagination could be attributed to its interference with different steps during placode morphogenesis. First, because we interfere with Rho function in pre-placodal stages, it is possible that lack of invagination was due to alteration of lens cell fate. This possibility was examined through assessment of Pax6 expression. Pax6 is expressed in pre-placode ectoderm cells and is required for progression of lens development (reviewed in Lang, 2004). Inhibition of Rho did not affect Pax6 expression (Fig. 5l). Alternatively, inhibition of Rho affects establishment of apical cytoskeleton in sea urchin and fly embryos and could be required for this role in the lens placode as well (Beane *et al.*, 2006; Dawes-Hoang *et al.*, 2005; Nikolaidou and Barrett, 2004). Thus, we examined the effect of C3 on the placode's actomyosin network. While C3 decreased slightly the apical/basal ratio of the actin-bound phalloidin fluorescent signal in relation to control (control: 100/22; experimental: 100/52; Fig. 5j,n), its effect was much more pronounced on myosin where the ratio changed from 100/46 to 91/100 (compare profiles in Fig. 5m,n). The results suggest that Rho activity is required for apical enrichment of myosin II but not of actin.

DISCUSSION

A comparative analysis of the previous publications on AC in various events of vertebrate epithelial morphogenesis identify some conserved elements as requirements for the establishment and progression of AC, namely accumulation of apical actomyosin, activation of myosin II, ROCK, Rho GTPase and Shroom 3 (Haigo

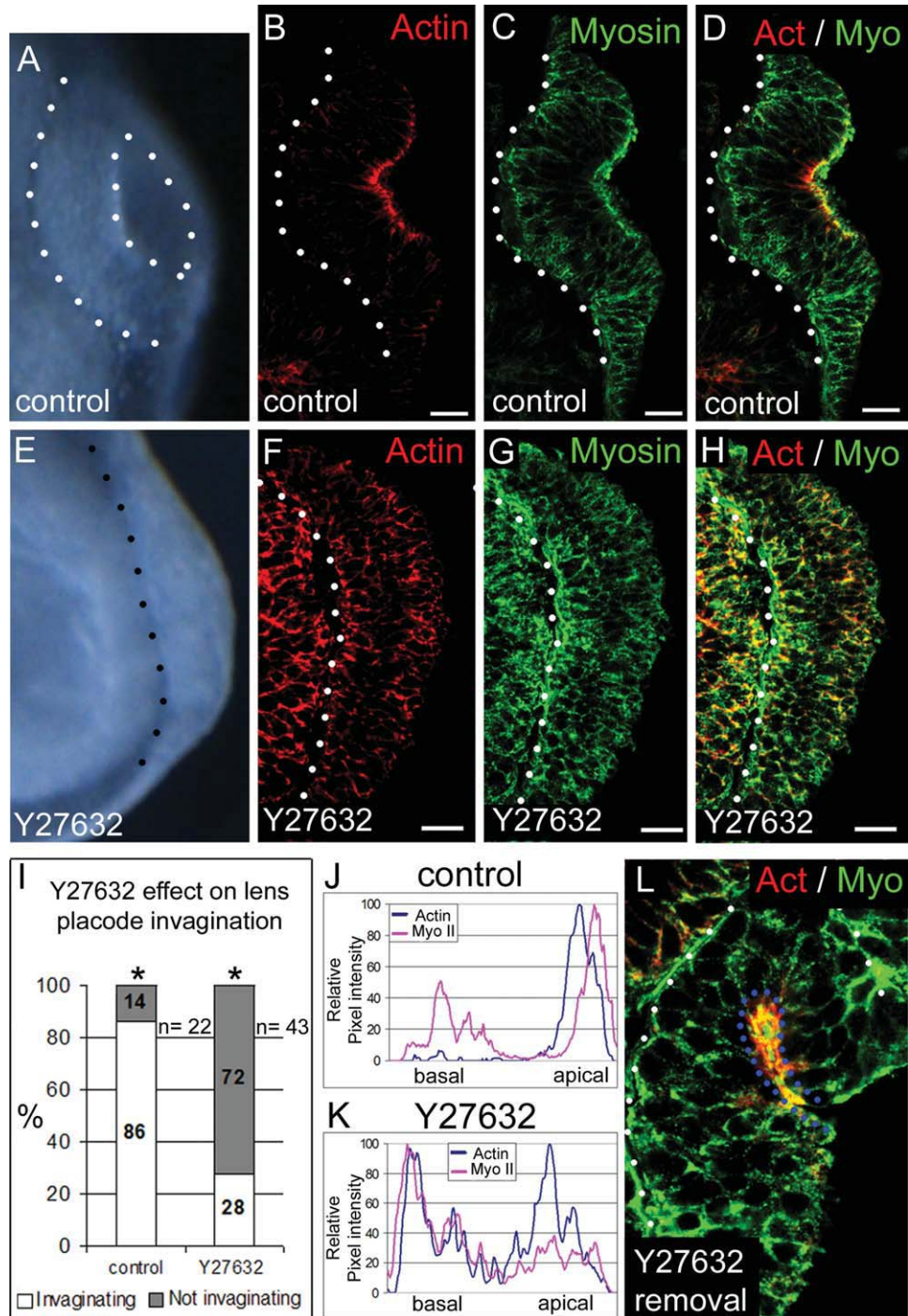


FIG. 4. ROCK activity is necessary for lens placode invagination and proper placement of the apical cytoskeleton. Cephalic explants were cultured in control media (a–d) or with 50 μ M Y27632 (e–h). The ROCK inhibitor decreased significantly the number of invaginating placodes (i) and suppressed apical accumulation of actin and myosin (compare k with j). After Y27632 treatment and inhibition of invagination, removal of the drug recovered placode invagination and apical positioning of actomyosin filaments (l, blue dotted line indicates lens pit). White dotted line delineates lens basal portion. Apical portion of all the placodes is to the right. Bar = 20 μ m. The difference between control and blebbistatin-treated embryos was statistically significant (*) with $P < 0.001$.

et al., 2003; Hildebrand, 2005; Kinoshita *et al.*, 2008; Plageman *et al.*, 2010). Here, we focused on the contribution of Rho-ROCK signaling pathway in the apical constriction of the early chick lens placode. Our data shows that apical RhoGTPases are involved in the establishment of the apical cytoskeleton prior to placode bending. The timing of the dynamics of RhoGTPases apical positioning in the early lens placode coincides with that of actin and myosin. Furthermore, inhibition of ROCK or Rho activity interfered with apical cytoskeletal distribution and abolishes lens invagination.

A detailed analysis of the cytoskeletal dynamics and its regulation during lens AC indicate that allocation of actin and myosin present differential requirement for Rho GTPases. Apical placement of myosin II in the lens placode was dependent both on Rho and ROCK activity. In contrast, polarized distribution of apical actin was a Rho-independent but ROCK-dependent event. Apical accumulation of actin in the chick neural plate is also impervious to C3-treatment (Kinoshita *et al.*, 2008). Thus, it seems that an alternative upstream element activates ROCK and determines the positioning of actin. A likely candidate is the actin-binding protein Shroom3 (Dietz *et al.*, 2006; Hildebrand and Soriano, 1999; Nishimura and Takeichi, 2008, Plageman *et al.*, 2010). Shroom3 interacts directly with actin through its ASD1 domain and overexpression of Shroom3 fragment containing this domain is sufficient to form ectopic actin bundles (Hildebrand and Soriano, 1999). Thus, it has been proposed that Shroom3 directly orchestrates the subcellular distribution of the actin cytoskeleton. This explanation could account for Rho-independent actin bundling, but does not address the alterations observed when we interfered with ROCK activity. In this sense, we propose that ROCK-dependent stabilization of actin at the apical surface depends indirectly on ROCK-mediated phosphorylation of myosin. Phosphorylated myosin II plays an important role in the maintenance of adhesive-junction-associated actin bundles (Shewan *et al.*, 2005). The question that remains is that of the signal that regulates apical myosin localization. Apical enrichment of myosin could be part of Rho-dependent polarization event that precedes Shroom3-mediated placodal invagination. In support of this, it is known that Shroom-induced apical constriction occurs only on previously polarized epithelia (Haigo *et al.*, 2003). This polarizing signal could be triggered by apical cadherins (Shewan *et al.*, 2005) or activation of the PAR complex (Nance *et al.*, 2003; Wang and Riechmann, 2007). Interestingly, as we show here, PAR-3 is apically enriched with the same dynamics as actin.

Thus, when we join our data with that of previously published results, one model that emerges involves a polarizing signal that activates Rho/ROCK to place unphosphorylated myosin II at the apical domain and also recruits Shroom3. The presence of Shroom3 in the

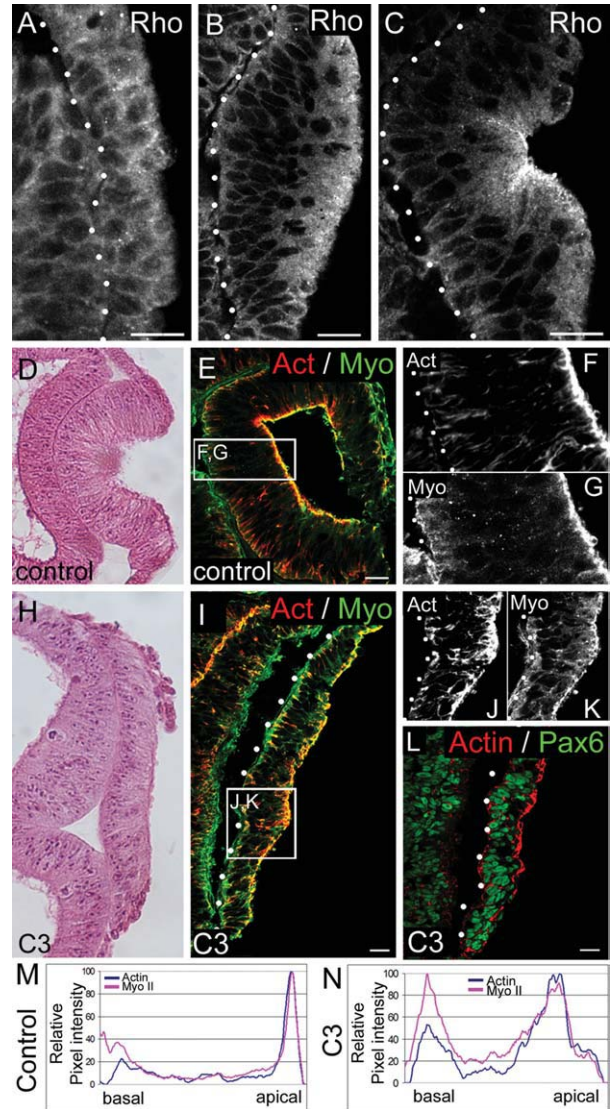


FIG. 5. Rho GTPase is expressed at the apical region of the placode and its activity is necessary for invagination. (a–c) Immunohistochemistry with a pan-Rho antibody in dorso-ventral sections of different stages of lens development: (a) pre-placode ectoderm; (b) early lens placode; (c) invaginating lens. Rho is homogeneously distributed at basal, lateral and apical cell sides at pre-placode ectoderm stage (a), becomes enriched apically at the lens placode stage (b) and remains concentrated apically during lens invagination (c). Hematoxylin-Eosin staining of C3 electroporated placodes (h) and its contralateral counterpart (d) showing that C3 overexpression inhibited lens placode invagination. Phalloidin-stained f-actin and immunohistochemistry to myosin II shows that C3 overexpression eliminated apical myosin II (i,k,n), but not apical f-actin accumulation (i,j,n: note that in actin staining, the apical portion has a stronger signal than the basal portion, and in the case of myosin II, both apical and basal portion show similar signal). Compare with f,g, where both actin and myosin are enriched apically when compared to basal portion of the invaginating lens. C3 does not alter placode expression of Pax6 (l). In all pictures, apical side of the lens is to the right, basal is to the left and dorsal is up. Dotted line indicates the interface with the basal lamina and the boxes delimit where quantification of pixel value was performed. Quantification of the pixel intensity for actin and myosin labeling confirms that apical enrichment of myosin is disrupted by C3 treatment (m,n). Bar = 20 μ m.

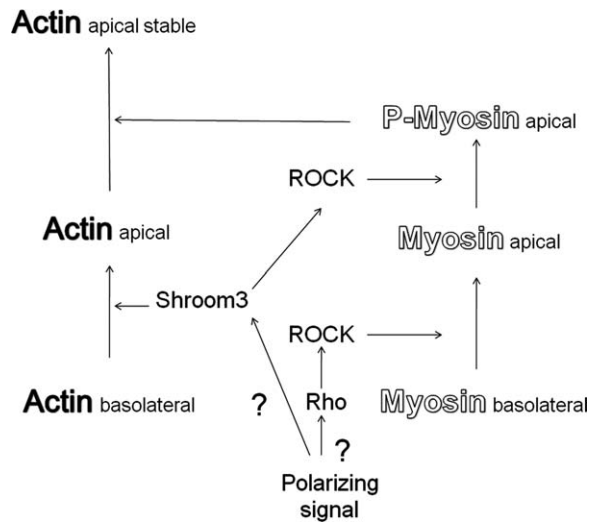


FIG. 6. Model of the role of Rho-ROCK pathway in the establishment of apical actomyosin cytoskeleton in the lens placode. Yet unidentified polarizing signals (possibly involving PAR proteins) convert the pre-placode ectoderm into a placode with distinct apico-basal domains and activate the Rho-ROCK pathway to place unphosphorylated myosin II at the apical domain. The established apical domain recruits Shroom3 which would then initiate polymerization of F-actin and bypass Rho to recruit ROCK and phosphorylate myosin, thus stabilizing apical actin and initiating apical contraction.

apical domain would then initiate apical accumulation of F-actin and also bypass Rho to recruit ROCK and phosphorylate myosin. Phosphorylation of myosin would stabilize apical actin and initiate apical contraction (see Fig. 6). Indeed, reduction of Shroom3 expression decreases apically located phosphorylated myosin in the chick neural tube and mouse lens placode (Nishimura and Takeichi, 2008; Plageman *et al.*, 2010). An alternative interpretation has been proposed by Hildebrand where Shroom3 alters myosin II localization indirectly through F-actin (Hildebrand, 2005). However, here we show that interference with RhoGTPase activity has a pronounced effect on myosin II distribution and a much milder effect on actin.

Our analysis of the cytoskeletal dynamics during placode formation also revealed that during placodal cell elongation there is a concomitant enrichment of actin and phosphorylated myosin II in the basal region. Although the levels of basal actin and myosin II are lower than in the apical subdomain, it is still significantly different from the remainder of the cell. A similar basal accumulation is observed in the mouse lens (Chauhan *et al.*, 2009).

The function of this basal pool of actin and myosin is currently unknown. In the mouse, the lens placode is connected to the underlying optic vesicle through interepithelial filopodia that transverse the distance between the two tissues. In this case, basal myosin II

has an active role in the contraction of placodal filopodia and contributes towards the transmission of mechanical force between invaginating optic cup and lens (Chauhan *et al.*, 2009; Wrenn and Wessels, 1969). However, interepithelial filopodia are not evident in the chick invaginating lens (Chauhan, personal communication; Schook, 1980a). Rather, the lens placode is in close apposition and firmly adhered to the underlying optic vesicle at stage HH10 to HH14 (McKeehan, 1951). One of the possibilities is that the basal actin-myosin network participates in this adhesive interaction through mature adhesions containing integrin complexes, as well as other structural and signaling proteins linked to the cytoskeleton (reviewed in Vicente-Manzanares *et al.*, 2009).

In conclusion, here we present data that confirm that apical constriction is a major driving force for lens placode invagination. However, given the complexity of the complete process of lens morphogenesis, it is possible that other mechanisms such as growth pressure or interaction with optic vesicle also contribute towards proper progression of the invagination and deserve to be investigated.

MATERIALS AND METHODS

Chick Embryo Staging and Cryosectioning

Eggs from Leghorn hens (Kunitomo Poultry Farm, Mogi das Cruzes, SP, Brazil) were incubated at 38°C with 50% humidity and collected by the filter-paper method (Chapman *et al.*, 2001) at different times after incubation, so as to obtain embryos at various morphological stages of development: pre-placode ectoderm (10–16 somites; HH10–12), lens placode (18–21 somites; HH12–13), or invaginating lens placode (22 somites; HH14) (Hamburger and Hamilton, 1951; McKeehan, 1951).

Embryos head were harvested by sectioning from the body above the heart level and cryoprotected in 20% sucrose at 4°C for 2 h. The explants were embedded in a 1:1 mixture of 20% sucrose and OCT (TissueTek) and frozen with dry ice. Heads were aligned so as to generate dorsoventral sections (10 μm). For Pax6 immunohistochemistry, the cephalic explants were pre-fixed in 4% paraformaldehyde for 5 min prior to embedding and cryosectioning as described above.

Immunohistochemistry on Frozen Sections

The slides were dried for 30 min at 37°C, fixed in 4% paraformaldehyde for 20 min, washed in PBS and blocked for 1 h with 3% NGS (Jackson ImmunoResearch) and 1% BSA (Jackson ImmunoResearch) diluted in PBST (PBS containing 0.1% Triton X-100—Sigma). Primary antibodies were diluted in PBST containing 3% NGS and applied on sections for 2 h at room temperature. The primary antibodies used were: rabbit anti-myosin

II (at $1.6 \mu\text{g ml}^{-1}$; Azevedo *et al.*, 2004—gift from Dr. Spreafico and Dr. Larson, University of São Paulo, Brazil); rabbit anti-MLC(phosphoSer19) (1:50, Cell Signaling Technology, USA no. 3671); rabbit anti-Rho (at $2 \mu\text{g ml}^{-1}$, Santa Cruz Biotechnology, USA no. sc-179); rabbit anti-Pax6 (1:250, Covance, USA no. PRB-278P); mouse anti-Beta-catenin (at $2.5 \mu\text{g ml}^{-1}$, BD Transduction Laboratories, USA no. 610153), and rabbit anti PAR-3 (1:50, Millipore, USA no. 07-330). Secondary antibodies used were Alexa 488-conjugated goat anti-rabbit (Molecular Probes, USA, dilution 1:1,000) or TRITC conjugated goat anti-mouse (Sigma, USA, dilution 1:100). For visualization of actin filaments, the previously immunostained cryosections were incubated for 30 min with rhodamine-phalloidin or phalloidin conjugated to Alexa488 fluorophore (Molecular Probes, USA, dilution of 1:100). Slides were mounted in Vecta Shield (Vector Laboratories, USA) and analyzed with a Nikon PCM2000 or Zeiss 510 Meta confocal microscopes or Nikon Eclipse e800 fluorescence microscope.

Quantification of Immunolabelling Fluorescence Intensity

The intensity of labeling for actin and myosin II was obtained by using the free imaging software Image J v 1.33 (NIH) to delimit a box on a section of the raw image data. The dimensions of the box were adjusted to encompass the apico-basal length of the tissue. The fluorescence intensity for all the pixels in the box along the apical-basal axis was added up (absolute intensity) and tabulated relative to its position along this axis (apico-basal distance). Thereafter the values were normalized to the highest absolute intensity value for each image. We attributed the value of 100 for the highest intensity and all other values were expressed as a fraction of this value. Thereafter, we always compared the ratio between highest normalized values in the apical/basal domain to obtain information regarding changes in relative distribution of acto-myosin cytoskeleton in these compartments. The quantification profiles shown are representative of at least three independent experiments.

In Ovo Actin Polymerization Inhibition (Cytochalasin D Treatment)

Chicken eggs were incubated until stages of 18–20 somites, when the lens placode is already formed but has not initiated invagination yet. The embryos were exposed *in ovo* by an opening in the eggshell and visualized under the stereomicroscope after contrasting with 10% Indian ink injection under the blastoderm (Selleck, 1996). Nitrocellulose fragments saturated with 1.5, 2.5, or $5 \mu\text{g ml}^{-1}$ Cytochalasin D diluted in DMSO (Sigma Aldrich) were applied over the developing placode. Eggs were then sealed with tape and reincubated for 6 h or until 22 somites stage, when lens pla-

code has invaginated in control embryos. Treated embryos where then dehydrated in an ethanol series, embedded in paraffin and sectioned ($4 \mu\text{m}$) for Hematoxylin-Eosin staining.

To verify whether CD treatment increased cell death, embryos previously treated with CD that did not have invaginating lens placode after reaching 22 somites stage were rinsed with Ringer's saline to remove CD, reincubated for 12 h and processed for paraffin sectioning and Hematoxylin-Eosin staining. Assessment of lens invagination inhibition was performed only at right lenses (that had the direct contact of CD) and are presented here as percentage of the total number of embryos treated. All placodes which presented a small indentation under stereoscope analysis were considered as invaginating.

In Ovo Electroporation

C3 exoenzyme (accession number X51464) clone was provided by Dr Fabio Forti (Forti and Armelin, 2007). Exoenzyme C3 was inserted into pEF-BOS and overexpressed by *in vivo* electroporation of the pre-placode ectoderm, as described in Momose *et al.*, 1999. Briefly, embryos were exposed *in ovo* and visualized with Indian ink injected under the blastoderm. The platinum electrodes (0.5-mm diameter) were placed flanking the head, at the level of the optic vesicles, with the negative electrode alongside the right lens placode. An aperture was made over the vitelline membrane at the same level and the embryos were bathed with Ringer's solution. Plasmid solution [$1\text{--}4 \mu\text{g } \mu\text{l}^{-1}$ in 0.1% Fast Green (Sigma)] was injected at the sub-cephalic pocket so as to bath the right eye, and five square pulses of 20 V and 50 ms of length and 100 ms of space were administered. Embryos were reincubated and analyzed 24 h later and processed for paraffin and frozen sectioning.

In Vitro Treatment With ROCK or Myosin II Inhibitors

Embryos at lens placode stage had their heads dissected above the heart with scissors and were maintained in ice cold Tyrode's solution before being cultured in 24-well plates (Falcon) coated with $300 \mu\text{l}$ of a medium containing 70% rat-tail collagen (extracted with 0.1% Glacial Acetic Acid, as described in Greene *et al.*, 1998), 10% of medium 199 (Gibco), 1M HEPES (Gibco), 1% of N2 supplement (Gibco), and 100 U ml^{-1} of penicillin/ $100 \mu\text{g ml}^{-1}$ streptomycin (Bailey *et al.*, 2006; Streit *et al.*, 1997). The pH was adjusted to 7.4 with 1M NaOH. Head explants were transferred to the collagen-coated wells with the right eye up and cultured in $200 \mu\text{l}$ of the same medium described above, except for the collagen, containing either $100 \mu\text{M}$ of the ROCK inhibitor Y27632 (Sigma) or $100 \mu\text{M}$ of the myosin II inhibitor blebbistatin (Sigma). Control explants were incubated

with medium only. The cultures were kept for 24 h at 38°C and 50% humidity, which was sufficient for the detection of placodal invagination in control explants.

For the invagination recovery experiment, the explants incubated with Y27632 had the medium changed for fresh medium without the drug and reincubated for additional 24 h.

ACKNOWLEDGMENTS

The authors are grateful to Enilza Espreafico for generously donating the antibodies to myosin II and Andrea Streit for sharing the cephalic explant culture protocol. They thank Chenbei Chang and Cristóvão de Albuquerque for critically reading the manuscript and Richard Lang for insightful discussions. They acknowledge Mr. José Antonio Turri's invaluable technical support.

LITERATURE CITED

- Afonso C, Henrique D. 2006. PAR3 acts as a molecular organizer to define the apical domain of chick neuroepithelial cells. *J Cell Sci* 119:4293–4304.
- Amano M, Ito M, Kimura K, Fukata Y, Chihara K, Nakano T, Matsuura Y, Kaibuchi K. 1996. Phosphorylation and activation of myosin by Rho-associated kinase (Rho-kinase). *J Biol Chem* 271:20246–20249.
- Azevedo A, Lunardi LO, Larson RE. 2004. Immunolocalization of myosin Va in the developing nervous system of embryonic chicks. *Anat Embryol (Berl)* 208:395–402.
- Bailey AP, Bhattacharyya S, Bronner-Fraser M, Streit A. 2006. Lens specification is the ground state of all sensory placodes, from which FGF promotes olfactory identity. *Dev Cell* 11:505–517.
- Barrett K, Leptin M, Settleman J. 1997. The Rho GTPase and a putative RhoGEF mediate a signaling pathway for the cell shape changes in *Drosophila* gastrulation. *Cell* 91:905–915.
- Baumann O. 2004. Spatial pattern of nonmuscle myosin-II distribution during the development of the *Drosophila* compound eye and implications for retinal morphogenesis. *Dev Biol* 269:519–533.
- Beane WS, Gross JM, McClay DR. 2006. RhoA regulates initiation of invagination, but not convergent extension, during sea urchin gastrulation. *Dev Biol* 292: 213–225.
- Burridge K, Wennerberg K. 2004. Rho and Rac take center stage. *Cell* 116:167–179.
- Byers B, Porter KR. 1964. Oriented microtubules in elongating cells of the developing lens rudiment after induction. *Proc Natl Acad Sci USA* 52:1091–1099.
- Chapman SC, Collignon J, Schoenwolf GC, Lumsden A. 2001. Improved method for chick whole-embryo culture using a filter paper carrier. *Dev Dyn* 220:284–289.
- Chauhan BK, Disanza A, Choi SY, Faber SC, Lou M, Beggs HE, Scita G, Zheng Y, Lang RA. 2009. Cdc42- and IRSp53-dependent contractile filopodia tether presumptive lens and retina to coordinate epithelial invagination. *Development* 136:3657–3667.
- Costa M, Wilson ET, Wieschaus E. 1994. A putative cell signal encoded by the folded gastrulation gene coordinates cell shape changes during *Drosophila* gastrulation. *Cell* 76:1075–1089.
- Dawes-Hoang RE, Parmar KM, Christiansen AE, Phelps CB, Brand AH, Wieschaus EF. 2005. folded gastrulation, cell shape change and the control of myosin localization. *Development* 132:4165–4178.
- Dietz ML, Bernaciak TM, Vendetti F, Kielec JM, Hildebrand JD. 2006. Differential actin-dependent localization modulates the evolutionarily conserved activity of Shroom family proteins. *J Biol Chem* 281:20542–20554.
- Donner AL, Lachke SA, Maas RL. 2006. Lens induction in vertebrates: Variations on a conserved theme of signaling events. *Semin Cell Dev Biol* 17:676–685.
- Forti FL, Armelin HA. 2007. Vasopressin triggers senescence in K-ras transformed cells via RhoA-dependent downregulation of cyclin D1. *Endocr Relat Cancer* 14:1117–1125.
- Fox DT, Peifer M. 2007. Abelson kinase (Abl) and Rho-GEF2 regulate actin organization during cell constriction in *Drosophila*. *Development* 134:567–578.
- Greene LA, Farinelli SE, Cunningham ME, Park DS. 1998. Culture and experimental use of the PC12 rat pheochromocytoma cell line. In: Banker G, Goslin K, editor. *Culturing nerve cells*. Cambridge: MIT Press. pp 161–187.
- Haigo SL, Hildebrand JD, Harland RM, Wallingford JB. 2003. Shroom induces apical constriction and is required for hinge-point formation during neural tube closure. *Curr Biol* 13:2125–2137.
- Hamburger V, Hamilton HL. 1951. A series of normal stages in the development of the chick embryo. *J Morphol* 88:49–92.
- Hendrix R, Madras N, Johnson R. 1993. Growth pressure can drive early chick lens geometries. *Dev Dyn* 196:153–164.
- Hildebrand JD. 2005. Shroom regulates epithelial cell shape via the apical positioning of an actomyosin network. *J Cell Sci* 118:5191–5203.
- Hildebrand JD, Soriano P. 1999. Shroom, a PDZ domain-containing actin-binding protein, is required for neural tube morphogenesis in mice. *Cell* 99:485–497.
- Kamisoyama H, Araki Y, Ikebe M. 1994. Mutagenesis of the phosphorylation site (serine 19) of smooth muscle myosin regulatory light chain and its effects on the properties of myosin. *Biochemistry* 33:840–847.
- Kinoshita N, Sasai N, Misaki K, Yonemura S. 2008. Apical accumulation of Rho in the neural plate is important for neural plate cell shape change and neural tube formation. *Mol Biol Cell* 19:2289–2299.
- Kovács M, Wang F, Hu A, Zhang Y, Sellers JR. 2003. Functional divergence of human cytoplasmic

- myosin II: Kinetic characterization of the non-muscle IIA isoform. *J Biol Chem* 278:38132-38140.
- Lang RA. 2004. Pathways regulating lens induction in the mouse. *Int J Dev Biol* 48:783-791.
- Lecuit T, Lenne PF. 2007. Cell surface mechanics and the control of cell shape, tissue patterns and morphogenesis. *Nat Rev Mol Cell Biol* 8:633-644.
- Lee JY, Harland RM. 2007. Actomyosin contractility and microtubules drive apical constriction in *Xenopus* bottle cells. *Dev Biol* 311:40-52.
- Liu JP, Jessell TM. 1998. A role for rhoB in the delamination of neural crest cells from the dorsal neural tube. *Development* 125:5055-5067.
- McKeehan MS. 1951. Cytological aspects of embryonic lens induction in the chick. *J Exp Zool* 117:31-63.
- Momose T, Tonegawa A, Takeuchi J, Ogawa H, Umeson K, Yasuda K. 1999. Efficient targeting of gene expression in chick embryos by microelectroporation. *Dev Growth Differ* 41:335-344.
- Nance J, Munro EM, Priess JR. 2003. *C. elegans* PAR-3 and PAR-6 are required for apicobasal asymmetries associated with cell adhesion and gastrulation. *Development* 130:5339-5350.
- Nikolaïdou KK, Barrett K. 2004. A Rho GTPase signaling pathway is used reiteratively in epithelial folding and potentially selects the outcome of Rho activation. *Curr Biol* 14:1822-1826.
- Nishimura T, Takeichi M. 2008. Shroom3-mediated recruitment of Rho kinases to the apical cell junctions regulates epithelial and neuroepithelial planar remodeling. *Development* 135:1493-1502.
- Pilot F, Lecuit T. 2005. Compartmentalized morphogenesis in epithelia: From cell to tissue shape. *Dev Dyn* 232:685-694.
- Plageman TF Jr, Chung MI, Lou M, Smith AN, Hildebrand JD, Wallingford JB, Lang RA. 2010. Pax6-dependent Shroom3 expression regulates apical constriction during lens placode invagination. *Development* 137:405-415.
- Popoff MR, Geny B. 2009. Multifaceted role of Rho, Rac, Cdc42, and Ras in intercellular junctions, lessons from toxins. *Biochim Biophys Acta* 1788:797-812.
- Sai X, Ladher RK. 2008. FGF signaling regulates cytoskeletal remodeling during epithelial morphogenesis. *Curr Biol* 18:976-981.
- Schook P. 1980a. Morphogenetic movements during the early development of the chick eye. An ultrastructural and spatial reconstructive study. A. Invagination of the lens placode. *Acta Morphol Neerl Scand* 18:133-157.
- Schook P. 1980b. Morphogenetic movements during the early development of the chick eye. An ultrastructural and spatial reconstructive study. B. Invagination of the optic vesicle and fusion of its walls. *Acta Morphol Neerl Scand* 18:159-180.
- Selleck MAJ. 1996. Culture and microsurgical manipulation of the early avian embryo. In: Bronner-Fraser M, editor. *Methods in avian embryology*. San Diego: Academic Press. pp 1-19.
- Shewan AM, Maddugoda M, Kraemer A, Stehbens SJ, Verma S, Kovacs EM, Yap AS. 2005. Myosin 2 is a key Rho kinase target necessary for the local concentration of E-cadherin at cell-cell contacts. *Mol Biol Cell* 16:4531-4542.
- Simoes S, Denholm B, Azevedo D, Sotillos S, Martin P, Skaer H, Hombria JC, Jacinto A. 2006. Compartmentalisation of Rho regulators directs cell invagination during tissue morphogenesis. *Development* 133:4257-4267.
- Straight AF, Cheung A, Limouze J, Chen I, Westwood NJ, Sellers JR, Mitchison TJ. 2003. Dissecting temporal and spatial control of cytokinesis with a myosin II inhibitor. *Science* 299:1743-1747.
- Streit A, Sockanathan S, Perez L, Rex M, Scotting PJ, Sharpe PT, Lovell-Badge R, Stern CD. 1997. Preventing the loss of competence for neural induction: HGF/SE, L5 and Sox-2. *Development* 124:1191-1202.
- Vicente-Manzanares M, Ma X, Adelstein RS, Horwitz AR. 2009. Non-muscle myosin II takes centre stage in cell adhesion and migration. *Nat Rev Mol Cell Biol* 10:778-790.
- Wang Y, Riechmann V. 2007. The role of the actomyosin cytoskeleton in coordination of tissue growth during *Drosophila* oogenesis. *Curr Biol* 17:1349-1355.
- Wilde C, Aktories K. 2001. The Rho-ADP-ribosylating C3 exoenzyme from *Clostridium botulinum* and related C3-like transferases. *Toxicon* 39:1647-1660.
- Wrenn JT, Wessells NK. 1969. An ultrastructural study of lens invagination in the mouse. *J Exp Zool* 171:359-367.